



Numerical simulation of thermal behavior and multicomponent mass transfer in direct laser deposition of Co-base alloy on steel



Zhengtao Gan, Gang Yu*, Xiuli He, Shaoxia Li

Key Laboratory of Mechanics in Advanced Manufacturing, Institute of Mechanics, Chinese Academy of Sciences, Beijing 100190, People's Republic of China

ARTICLE INFO

Article history:

Received 14 April 2016

Accepted 13 August 2016

Keywords:

Laser cladding

Thermal behavior

Solidification

Multicomponent mass transfer

ABSTRACT

During direct laser deposition process, rapid melting–solidification and addition of multicomponent powder lead to complex transport phenomena in the melt pool. The thermal behavior and mass transport significantly affect the solidified microstructure and properties of fabricated layer. In this paper, an improved 3D numerical model is proposed to simulate the heat transfer, fluid flow, solidification and multicomponent mass transport in direct laser deposition of Co-base alloy on steel. The solidification characteristics, including temperature gradient (G), solidification growth rate (R) and cooling rate ($G \times R$), can be obtained by transient thermal distribution to predict the morphology and scale of the solidification microstructure. Multicomponent transport equation based on a mixture-averaged approach is combined with other conservation equations. The calculated melt pool geometry and the composition profiles of iron (Fe), carbon (C), cobalt (Co) and chromium (Cr) are compared with the experimental results. The results show that in the initial stage of direct laser deposition, the rapidly mixture of substrate material and added material occur in the melt pool and conduct plays an important role in heat transfer due to the low Peclet number. As the melt pool is developed, the heat and mass transfer in the melt pool are dominated by strong Marangoni convection. An unmixed zone is observed near the bottom of melt pool where the convection is frictionally dissipated due to the presence of solidified dendrites. Since the G/R decreases and $G \times R$ increases from the bottom to the top of the solidified track, the morphology of the microstructure changes from planar front to columnar dendrites to equiaxed dendrites and the grain size decreases.

© 2016 Elsevier Ltd. All rights reserved.

1. Introduction

Direct laser deposition, as an advanced additive manufacturing technology, provides an attractive tool to fabricate functionally gradient materials. It has some benefits compared with the traditional surface modification and manufacture technique, such as its small heat affected zone, low thermal strain, low porosity, and finer grain size [1,2]. In direct laser deposition, the substrate is melted by a high power density laser beam creating a melt pool in which the multicomponent alloy powders are injected [3]. Co-base and Ni-base alloy have been widely used as the added material to improve the surface properties of substrate, such as strength, wear resistance and corrosion resistance [4–6]. In spite of its widespread application, an understanding of transport phenomena and solidification behavior in the melt pool still remains as a challenge.

During this process, metallic powders addition into the melt pool result in the redistribution of alloy elements in the melt pool [7,8]. Due to the difference in chemical composition and thermo-physical property of substrate and added material, a great deal of defects, involving the non-fusion owing to insufficient heat transfer, the formation of brittle intermetallic compound and low melting point eutectics owing to inappropriate solute transport, all make the deposited layer prone to crack and failure [9,4,10]. Selecting appropriate composition of powder material and thermo-physical property is an approach to overcome the problem and obtain ideal deposited layer properties. However, a large number of trial experiments are time-consuming and money-consuming. Numerical simulation has offered an effective tool in prediction the thermal behavior and mass transport in direct laser deposition [11–22]. A three-dimensional mathematical model has been established in which the temperature field and flow field is obtained [11]. In order to simulate mass addition process, the level set approach was introduced into the numerical model to capture the liquid/gas interface of melt pool. The direct metal deposition was studied by a 3D numerical model [12]. The transport phenom-

* Corresponding author.

E-mail address: gyu@imech.ac.cn (G. Yu).

ena including heat transfer and fluid flow were investigated and analyzed. Kumar et al. [13] proposed and solved sets of dimensionless transport equations to investigate the laser metal deposition process. Deposited track geometry, dilution rate and maximum melt pool temperatures were calculated. Lee et al. [14] developed a three-dimensional transport model to understand the melt pool formation, liquid metal flow and the evolution of surface tension in Inconel 718 laser deposition.

The heat transfer affects the solidification behavior of deposited track. Few studies tried to obtain the solidification characteristics of deposited track depending on computed temperature distribution. A 3D thermal FEM model has been built to calculate the temperature variation, the cooling rate and the solidifying rate in the solid–liquid interface [15]. Using a Fourier heat conduction model, the effect of substrate temperature and cooling rates on the distribution of added particles was investigated [16]. However, the Marangoni convection caused by the thermocapillary effect did not consider in these numerical models.

Although numerical simulation has previously offered a tool of effective evaluating the thermal behavior during the direct laser deposition process [11–18], few models considered the mass transfer in this process. Huang et al. [19] studied the heat and mass transport during the laser metal deposition process. The dual-equation of mass transfer was utilized to calculate separately the composition profile between deposited layer and base metal. He et al. [20,21] proposed a 3D transient heat and mass transfer model to predict the solute distribution in the deposited layer. The mathematical model was calculated by solving the species conservation equations besides the energy and momentum conservation equations. The binary system Fe–C and Fe–Cr were evaluated to obtain the concentration distribution of C and Cr [20]. The solute transfer and composition profiles evolution for binary system Fe–C during double-track direct metal deposition also have been reported [21]. Although the multicomponent mass transfer model has been built in metal casting and chemical engineering [22,23], such study for direct laser deposition has not been reported in the open peer-reviewed literature.

In this paper, a self-consistent model, including thermal behavior, liquid metal flow, solidification and multicomponent mass transfer, are investigated in direct laser deposition. The temperature gradient (G) and solidification growth rate (R) are obtained by thermal analysis to predict the morphology and scale of the solidification microstructure. To consider the multicomponent convection and diffusion in the movable melt pool, multicomponent transport equation based on a mixture-averaged approach is combined with the equations of mass, momentum and energy conservation. The composition profiles of iron (Fe), carbon (C), cobalt (Co) and chromium (Cr) in the deposited track are also present. The computed melt pool geometry and composition profiles are compared with the experimental results. The present study demonstrates the numerical simulation of transport phenomena can generate significant insight into details of thermal behavior and multicomponent mass transport in direct laser deposition.

2. Experimental procedure

38MnVS medium carbon steel and Co-base alloy powder are selected as substrate and added material. Table 1 shows the com-

Table 1
Material composition of 38MnVS carbon steel and Co–Cr–W powder (weight %).

	Fe	C	Co	Mn	Cr	W	V	S
38MnVS	Bal	0.38	–	1.4	0.16	–	0.5	0.04
Co–Cr–W	–	0.35	Bal	1.8	20	3	–	–

positions of material. Fig. 1 shows the schematic diagram of experimental setup. Direct laser deposition was implemented on a 1000 W Nd: YAG laser manufacturing system with six-axis programmed control platform. The focal length of lens is 160 mm. The pattern of laser beam is multi-mode and the beam radius is set to 1 mm (defocus of beam is 10 mm). Two feeding pipes are used to delivery powder into melt pool. High purity argon is used as shielding gas. Samples of the substrate were prepared in the size of 20 mm × 10 mm × 6 mm. Metallographic samples were prepared by electric discharge cutting, mechanical milling and grinding, followed by standard mechanical polishing and then etched in aqua regia solution. In order to examine the solidified microstructure and concentration of alloy element, the samples were characterized by JSM-6460 scanning electron microscopy (SEM) equipped with Oxford INCA energy dispersive spectrometer (EDS).

3. Mathematical model

A mathematical model involving heat transfer, fluid flow and mass transfer in direct laser deposition is proposed. The simplifying assumptions are the following [11,20]:

1. The fluid flow in the melt pool is assumed to be Newtonian, laminar and incompressible.
2. The thermophysical properties of powder and substrate are assumed to be temperature-independent.
3. The laser heat flux is assumed to be a Gaussian distribution.
4. The heat flux of the heated powder and the heat loss by evaporation are neglected.
5. The mushy zone where the temperature is between the solidus and liquidus is assumed as a porous medium with isotropic permeability.
6. There is no diffusion transport in solid phase.
7. The concentration distribution of powder flow is assumed to be Gaussian. Powders falling in the region of melt pool are melted immediately.
8. The energy attenuation of laser beam through the powder flow is neglected.

3.1. Governing equations

The equations of conservation of mass, momentum-transport, thermal energy and species concentration are formulated as Eqs. (1)–(4).

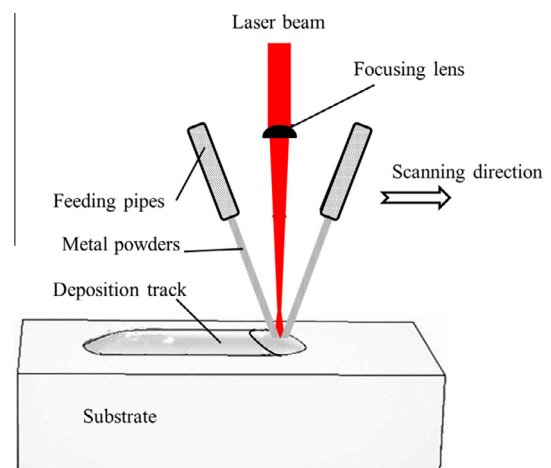


Fig. 1. Schematic diagram of experimental setup for direct laser deposition.

Download English Version:

<https://daneshyari.com/en/article/656320>

Download Persian Version:

<https://daneshyari.com/article/656320>

[Daneshyari.com](https://daneshyari.com)